



## OPEN

SUBJECT AREAS:  
ROOT APICAL MERISTEM  
PLANT PHYSIOLOGYReceived  
18 September 2014Accepted  
12 January 2015Published  
5 February 2015Correspondence and  
requests for materials  
should be addressed to  
J.L. (lijsh2011@163.  
com)

# Hydrogen sulfide modulates actin-dependent auxin transport via regulating ABPs results in changing of root development in Arabidopsis

Honglei Jia<sup>1</sup>, Yanfeng Hu<sup>2</sup>, Tingting Fan<sup>3</sup> & Jisheng Li<sup>1</sup>

<sup>1</sup>College of Life Sciences, Northwest A&F University, Yangling, Shaanxi 712100, China, <sup>2</sup>Key Laboratory of Mollisols Agroecology, Northeast Institute of Geography and Agroecology, Chinese Academy of Sciences, Nangang District, Harbin 150000, China, <sup>3</sup>School of Biotechnology and Food Engineering, Hefei University of Technology, Hefei, Anhui 230009, China.

Hydrogen sulfide (H<sub>2</sub>S) signaling has been considered a key regulator of plant developmental processes and defenses. In this study, we demonstrate that high levels of H<sub>2</sub>S inhibit auxin transport and lead to alterations in root system development. H<sub>2</sub>S inhibits auxin transport by altering the polar subcellular distribution of PIN proteins. The vesicle trafficking and distribution of the PIN proteins are an actin-dependent process. H<sub>2</sub>S changes the expression of several actin-binding proteins (ABPs) and decreases the occupancy percentage of F-actin bundles in the Arabidopsis roots. We observed the effects of H<sub>2</sub>S on F-actin in T-DNA insertion mutants of *cpa*, *cpb* and *prf3*, indicating that the effects of H<sub>2</sub>S on F-actin are partially removed in the mutant plants. Thus, these data imply that the ABPs act as downstream effectors of the H<sub>2</sub>S signal and thereby regulate the assembly and depolymerization of F-actin in root cells. Taken together, our data suggest that the existence of a tightly regulated intertwined signaling network between auxin, H<sub>2</sub>S and actin that controls root system development. In the proposed process, H<sub>2</sub>S plays an important role in modulating auxin transport by an actin-dependent method, which results in alterations in root development in Arabidopsis.

Auxin was the first identified phytohormone, and it plays a critical role in a variety of physiological and developmental processes in plants, including apical dominance, inflorescence and phyllotaxis development, embryogenesis, root development, lateral root (LR) and adventitious root initiation, tropism and vascular differentiation<sup>1</sup>. These processes depend on the establishment of auxin concentration gradients coordinated by auxin biosynthesis and polar auxin transport (PAT). Auxin is mainly synthesized in young aerial tissues and roots, particularly in the meristematic part of root apices<sup>2</sup>. From the auxin source in the shoot, plants transport indole acetic acid (IAA) to the basal tissues (e.g., the root) in a process that is dependent on the specialized PAT<sup>3</sup> delivery system. In the root, PAT moves IAA to the root-shoot junction (basipetal) and towards the root apex (acropetal)<sup>4,5</sup>. Establishment of an auxin gradient with its maximum at the root apex is important for primary root growth and for LR development<sup>3,6</sup>.

PAT is mediated by auxin influx carriers from the AUXIN RESISTANT 1/LIKE-AUX1 (AUX1/LAX) protein family, and by auxin efflux proteins from the PIN-FORMED (PIN) family and the ATP-binding cassette protein B/multi-drug resistance/P-glycoprotein (ABCB/PGP/MDR) subfamily<sup>7</sup>. It has been reported that IAA is taken up into cells via AUX/LAX permeases through the ATP-dependent proton-driven anionic (IAA<sup>-</sup>) symport and MDR/PGP-type ABC transporters<sup>8-10</sup>. Recent studies have revealed that PINs regulate the auxin maxima in the distal domains of organ primordia<sup>11,12</sup>. Auxin efflux carrier PIN2 regulates the root gravitropism and the basipetal auxin transport in Arabidopsis roots<sup>13</sup>. In addition, the Arabidopsis *pin3pin4pin7* triple mutant shows reduced LR<sup>14</sup>. Much data indicates that PINs are important regulators of PAT and root development<sup>11,13-15</sup>.

PAT is an actin-dependent process because the vesicle trafficking of PIN proteins requires the actin cytoskeleton<sup>16</sup>. A functional and intact actin cytoskeleton is necessary for root growth in Arabidopsis<sup>6</sup>. The actin cytoskeleton affects the subcellular dynamics of PIN proteins and impairs auxin efflux out of cells and auxin transport<sup>17</sup>. In response to these critical processes, the actin cytoskeleton needs to be rapidly and dramatically changed into different structures, and this organization is precisely controlled by various actin binding proteins



(ABPs), including profilin, ADF/confilin, fimbrin, villin, formin, and myosin<sup>18</sup>. It is reported that ABPs are essential for the development of plant structures such as root hair<sup>19</sup>, primary root<sup>20</sup>, hypocotyl<sup>21</sup>, and pollen tubes<sup>22</sup>. In addition, the functions of ABPs were shown to be regulated by a variety of signaling molecules, including pH, PIP<sub>2</sub>, Ca<sup>2+</sup> and PA<sup>23,24</sup>.

Hydrogen sulfide (H<sub>2</sub>S) is a colorless gas that has been considered toxic for many years. However, the biological effects of H<sub>2</sub>S have only been recently recognized. It seems that this gas is not only the agent potentially responsible for past mass extinctions but is also an important signaling molecule<sup>25,26</sup>. Furthermore, H<sub>2</sub>S was identified as the third endogenous gaseous transmitter, following the discovery of nitric oxide (NO) and carbon monoxide (CO)<sup>27</sup>. In plant systems, the mechanisms of H<sub>2</sub>S synthesis and release have been characterized for a long time<sup>28</sup>. However, very few studies have focused on the biology of H<sub>2</sub>S in plants. Only recently, the positive effects of H<sub>2</sub>S in response to the abiotic stress in plants, such as osmotic stress<sup>29</sup>, salt stress<sup>30</sup>, heat shock stress<sup>31</sup> and heavy metal stress, have been studied<sup>32</sup>. H<sub>2</sub>S is also involved in the growth and development of plants. Many studies have shown that H<sub>2</sub>S is involved in stomatal closure, seed germination and increasing the growth rate<sup>33,34</sup>.

Recently, it has been reported that H<sub>2</sub>S can interact with IAA and can regulate the adventitious root and the LR formation in batatas and tomato plants<sup>30,35</sup>. However, the specific response mechanisms of the root development are less clear. In the present study, the interrelation between H<sub>2</sub>S and auxin on the root system growth was investigated. We provide evidence that H<sub>2</sub>S affects auxin distribution and transport by regulating the actin cytoskeleton in the Arabidopsis root.

## Results

**H<sub>2</sub>S inhibits primary root, LR and root hair elongation but promotes LR initiation in WT seedlings.** It has been indicated that H<sub>2</sub>S is a secondary signal molecule that acts in response to the growth and development of plants<sup>25,26</sup>. The exogenous application of H<sub>2</sub>S donors was able to alter the endogenous H<sub>2</sub>S levels in a dose-dependent manner in Arabidopsis roots (Fig. 1a) and in other plants, such as maize and strawberry<sup>21,29</sup>. Changing the endogenous H<sub>2</sub>S levels can affect the root system architecture<sup>36</sup>. However, our knowledge of the molecular mechanisms by which way H<sub>2</sub>S regulates growth and development in Arabidopsis remains fragmentary.

To investigate the role of H<sub>2</sub>S in the regulation of primary root growth in Arabidopsis, WT (*Arabidopsis thaliana* ecotype Columbia-0, Col-0) plants were germinated on plates containing different concentrations of H<sub>2</sub>S released by the H<sub>2</sub>S donor - sodium hydrosulfide (NaHS) or GYY4137. As shown in Fig. 1, b & c, the inhibition was dose dependent, because a gradual decrease in the length of the primary root (from 1.5 ± 0.1 to 0.4 ± 0.1 cm) was observed as the NaHS levels increased from 0–500 μM. To validate our results by using other H<sub>2</sub>S donors, we tested GYY4137. The inhibition of primary root growth had a similar effect (59.8% inhibition in 100 μM GYY4137 treatment and 20.2%–72.1% inhibition under 50–500 μM NaHS treatments, respectively).

LR and root hairs, which typically constitute the majority of the root systems in plants, contribute greatly to nutrient acquisition from soil; the development of these structures are regulated by many signaling molecules<sup>37</sup>. We examined the effect of H<sub>2</sub>S treatment on LR initiation and elongation. Considering these two developmental regions independently, we examined the effects of H<sub>2</sub>S on the lateral root primordium (LRP) and the LR, respectively. According to the anticlinal divisions and the cell expansion and periclinal divisions, the LRP development is grouped into I to III, IV to VII and emergence<sup>38</sup>. We observed an increase in the LRP initiation events when the 3-d-old seedlings were transferred onto NaHS. The density of the LRPs increased at 100 μM NaHS in all stages (I to III, IV to VII and

emergence). At higher doses of NaHS, the number of LRP initiation events increased in a concentration-dependent manner (Fig. 2b). Thus, the effect of H<sub>2</sub>S on LRP initiation was not specific for any particular stage. An increased number of LR were observed in the 3-d-old seedlings transferred onto NaHS at 4 d, but the length of the LR was inhibited by NaHS (Fig. 2c & d). These results indicate that the effects of H<sub>2</sub>S on the initiation and growth of the LR are different.

The root hair density and the root hair length dramatically decreased following treatment with 50 to 200 μM NaHS for 24 to 48 h (Fig. S1). The application of GYY4137 had the same effect as NaHS (Fig. S1). In addition, we found that when treated with NaHS, the germination time of the seeds was significantly shorter in contrast with the untreated seeds (Fig. S2). Together, the pharmacological data suggest that H<sub>2</sub>S plays an important role in Arabidopsis root system development, inhibiting the primary root, LR and root hair development while promoting LR initiation.

## H<sub>2</sub>S alters auxin response patterns and inhibits auxin transport in WT.

Auxin response patterns based on auxin gradients are important factors in the regulation of many developmental processes, including cell division, elongation, and differentiation during primary root growth<sup>6</sup>. As an indicator of the auxin response, *DR5::GUS* is expressed in the root apex and during LR initiation<sup>13</sup>. *DR5::GUS* expression was assayed by histochemical staining and a quantitative assay of GUS activity. The control showed that *DR5::GUS* is expressed in the quiescent center (QC), columella initial cells and mature columella cells of the root apex (Fig. 3a). *DR5::GUS* expression could be attenuated in the three layers of columella cells and confined to the QC by increasing the H<sub>2</sub>S levels after application of NaHS (Fig. 3a). After treatment with 200 μM NaHS or 100 μM GYY4137 for 12 or 24 h, the expression of *DR5::GUS* gene was also markedly inhibited (Fig. 3a). To further validate our results, the GUS activity was quantified. As shown in Fig. 3b & c, the GUS activity decreased in a dose-dependent and time-dependent manner after NaHS application. In addition, GYY4137 had the same effect as NaHS on the GUS activity.

In Arabidopsis, LRP initiate exclusively from the pericycle founder cells, which are located opposite from xylem poles. Pericycle founder cells undergo several rounds of anticlinal divisions to create a single layered primordia composed of up to ten small cells of equal length (stage I). These cells divide periclinal, forming an inner and an outer layer (stage II). Further periclinal and anticlinal divisions set up a dome-shaped primordium (stages III–VII) that eventually emerge from the new LR (the emergence stage).

We next examined the distribution of auxin in several stages of LR development in the *DR5::GUS* transgenic seedlings following NaHS treatment. In the control seedlings, the site of LRP initiation (stages I–III) had the maximal *DR5::GUS* expression accumulation. A high level of *DR5::GUS* expression was observed in the next stages of LR development (stages IV–VII), which included the formation and emergence of the LRP (Fig. 3d). The results indicated that the entire developmental stage of LR required the maintenance of auxin distribution. In the NaHS-treated seedlings, no significant modifications in the *DR5::GUS* expression were observed over the stages of LR development (stages I–VII and emergence) compared to the untreated plants. However, the NaHS treatment markedly decreased the *DR5::GUS* activity in the apex of the mature LR (Fig. 3d).

The observed change in the *DR5::GUS* expression pattern implies that auxin transport might be altered by increasing the endogenous H<sub>2</sub>S levels. To assess this hypothesis, we tested the acropetal and basipetal auxin transport in the roots of WT samples using [<sup>3</sup>H]-IAA. We used the untreated seedlings as the normalized samples and defined their value as 100% (Fig. 4). The normalized data showed that treatment with NaHS or GYY4137 markedly altered the auxin transport. A drastic reduction in acropetal and basipetal auxin movement was detected following NaHS and GYY4137 treatment (Fig. 4a

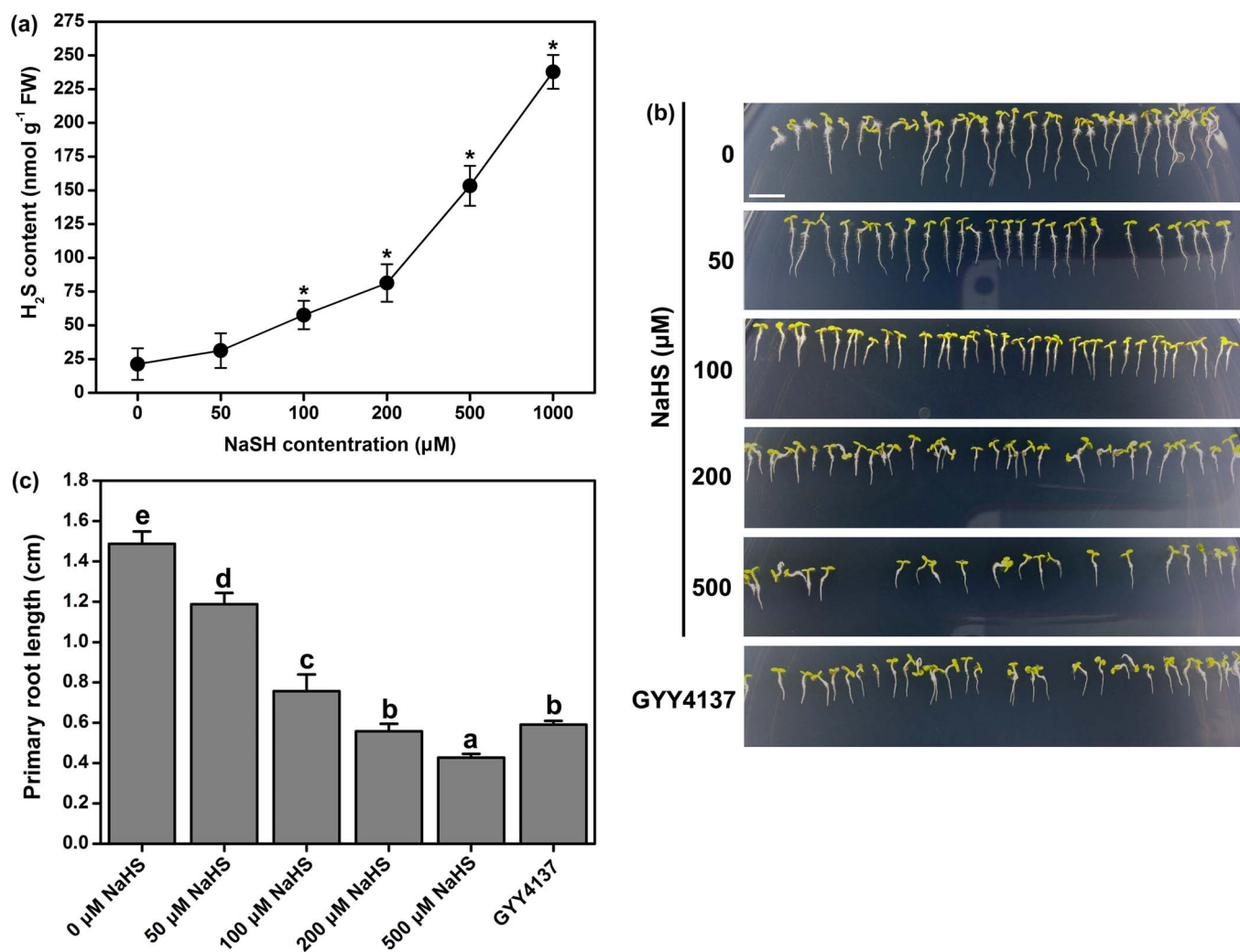


**Figure 1 | Effects of NaSH on endogenous H<sub>2</sub>S content in the root of WT Arabidopsis.** (a) 5-d-old Arabidopsis seedlings were transferred to the 1/2 MS agar medium. Effects of NaSH on endogenous H<sub>2</sub>S content in Arabidopsis root. 50–1000 µM NaHS were used for various treatments for 6 h. (b) Effect of H<sub>2</sub>S in the regulation of primary root growth in WT Arabidopsis. Photograph showing the length of primary root of WT Arabidopsis seedlings. 3-d-old seedlings were transferred to 1/2 MS agar plates grown for 2 d. The agar plate were untreated (Control) or supplemented with 50 µM, 100 µM, 200 µM, or 500 µM of NaHS or supplemented with 200 µM GYY4137. Scale bar = 1 cm. (c) The length of primary root were obtained 2 d after the treatment of 3-d-old seedlings. Mean values and SE are calculated from three replicates in (a). Data are mean values and SE (n > 25) in (b) and (c). Within each set of experiments, bars with different letters are significantly different ( $P < 0.05$ , Duncan's multiple range tests).

& b). In addition, both the acropetal and basipetal auxin transport were decreased by NAP (Fig. 4a & b). These data supported the hypothesis that enhanced H<sub>2</sub>S levels cause a defect in the IAA transport capacity.

**H<sub>2</sub>S alters the subcellular localization of PIN1, PIN2, PIN4 and PIN7 in the root apices.** The PIN proteins are important regulators in the establishment stage and in the auxin gradient in plants<sup>11</sup>. The polar subcellular localization of the PIN proteins at the plasma membrane determines the directionality of auxin flow<sup>40</sup>, thus contributing to regulation of multiple aspects of plant development<sup>41</sup>. Therefore, we examined the fluorescence of GFP fusions to PINs in Arabidopsis roots to determine if H<sub>2</sub>S could regulate the subcellular localization of the PIN proteins. The PIN proteins were clearly visible in the plasma membrane and showed a polar distribution in the control seedlings (Fig. 5). Treatment with NaHS or GYY4137 for 6 h showed the loss of their polar distribution at the plasma membrane in the root epidermal cells. Notably, a substantial amount of the PIN:GFP signal dissociated from the plasma membrane upon cytoplasmic entry (Fig. 5). In addition, the fluorescent intensity of

PIN1:GFP, PIN2:GFP, and PIN7:GFP increased after the roots were treated with NaHS or GYY4137 for 6 h in root epidermal cells (PIN1 increased from 25.3% and 11.2% in response to NaHS and GYY4137, respectively; PIN2 increased from 87.2% and 53.9%; PIN7 increased from 35.6% and 25.9%, Fig. 5b). In contrast, the fluorescent intensity of PIN4:GFP decreased (by 24.7% and 30.6% after NaHS and GYY4137, respectively, Fig. 5b). The localization of PIN1 and PIN2 were observed in the *cpa*, *cpb*, *pfr3* mutants (Fig. S7). The plasma membrane localization of PIN1 and PIN2 was similar between the ABP mutants and the WT samples. After treatment with NaHS for 6 h, the PIN1 localization was altered in both the ABP and WT samples. In contrast, the localization of PIN2 also changed following 6 h NaHS treatment in the *cpa* and *pfr3* mutants and the WT samples. While the localization in the *cpb* mutant did not immediately change, after treatment with NaHS for 12 h, the PIN2 localization was altered in both ABP mutants and WT (Fig. S7).

qRT-PCR analysis of the expression of *PIN1*, *PIN2*, *PIN3*, *PIN4* and *PIN7* in the WT root showed that *PIN1*, *PIN2* and *PIN7* increased after treatment with NaHS for 3 to 6 h (Fig. S3). *PIN1* was recovered to the control levels by 6 h, and the expression of

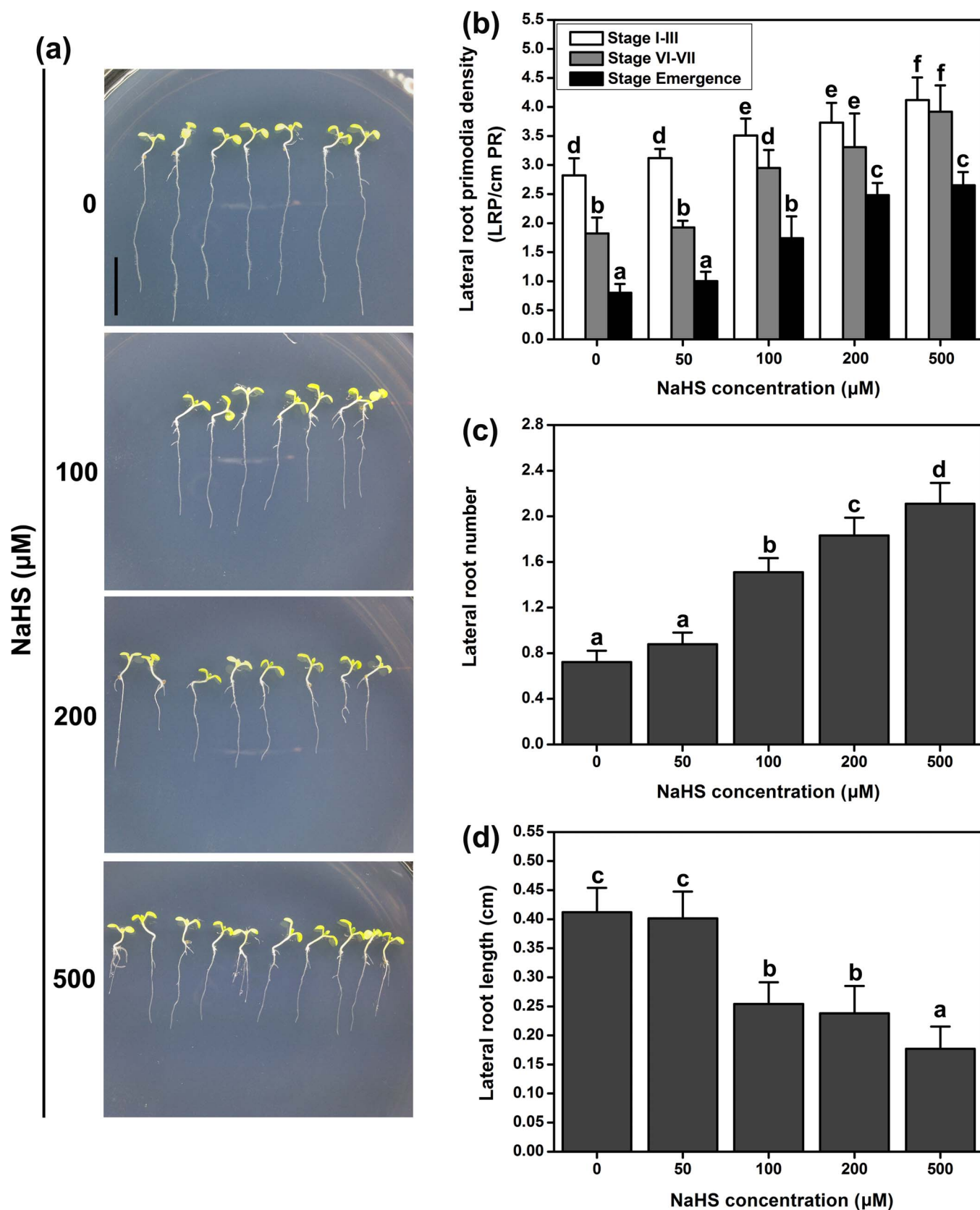


**Figure 2 | Effect of  $\text{H}_2\text{S}$  on LR initiation and growth.** (a) Effect of  $\text{H}_2\text{S}$  in the regulation of LR growth in WT Arabidopsis. Photograph showed that 3-d-old seedlings were transferred to 1/2 MS agar plates grown for 4 d. (b) The density of LR primordia. Different stages of LRP (stages I–VII, emergence) were scored. 3-d-old WT seedlings were grown on agar plates supplied with 0–500  $\mu\text{M}$  NaHS for 4 d. (c) The number of LP were obtained 4 d after the treatment of 3-d-old seedlings. (d) The length of LP were obtained 4 d after the treatment of 3-d-old seedlings. Data are mean values and SE ( $n > 25$ ) in (b), (c) and (d). Within each set of experiments, bars with different letters are significantly different ( $P < 0.05$ , Duncan's multiple range tests).

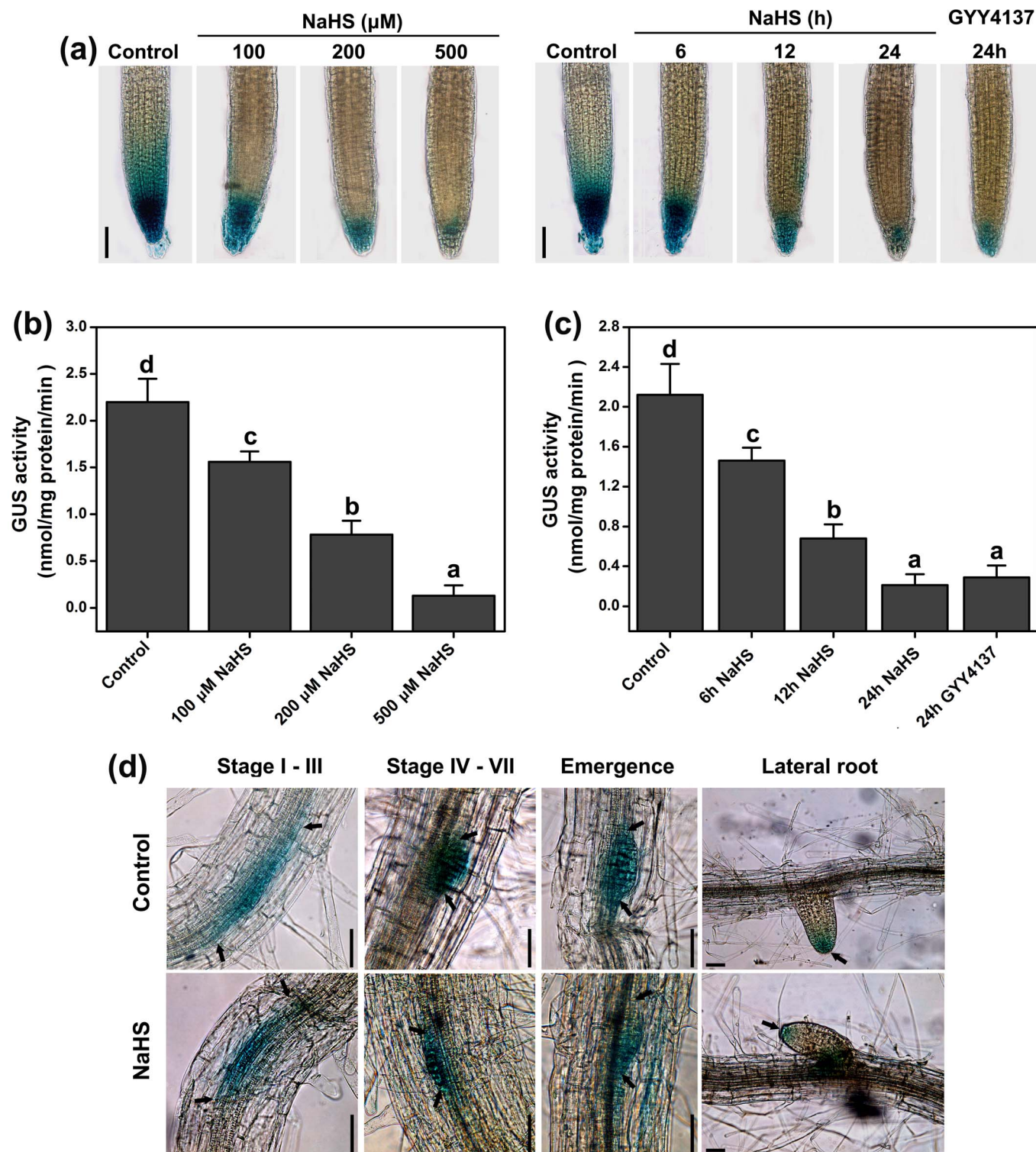


**Figure 3** | Effects of  $\text{H}_2\text{S}$  on the auxin level of *Arabidopsis* root monitored by *DR5::GUS*. (a) Histochemical GUS staining patterns of *DR5::GUS* in 5-d-old seedlings treated with 100–500  $\mu\text{M}$  NaHS for 12 h. Histochemical GUS staining patterns of *DR5::GUS* in 5-d-old seedlings treated with 200  $\mu\text{M}$  NaHS and 100  $\mu\text{M}$  GY4137 for various time. Scale bar = 100  $\mu\text{m}$ . (b) GUS activity of *DR5::GUS* in 5-d-old seedlings treated with 100–500  $\mu\text{M}$  NaHS for 12 h. (c) GUS activity of *DR5::GUS* in 5-d-old seedlings treated with 200  $\mu\text{M}$  NaHS and 100  $\mu\text{M}$  GY4137 for various time. (d) Expression pattern of *DR5::GUS* in LRP. 5-d-old *Arabidopsis* *DR5::GUS* seedlings were grown on agar plates supplied with solvent (Control) or 200  $\mu\text{M}$  NaHS for 0–48 h. Images shown are representative of each treatment. Scale bar = 50  $\mu\text{m}$ . Mean values and SE are calculated from three replicates in (b) and (c). Data are mean values and SE ( $n > 25$ ) in (a) and (d). Within each set of experiments, bars with different letters are significantly different ( $P < 0.05$ , Duncan's multiple range tests).

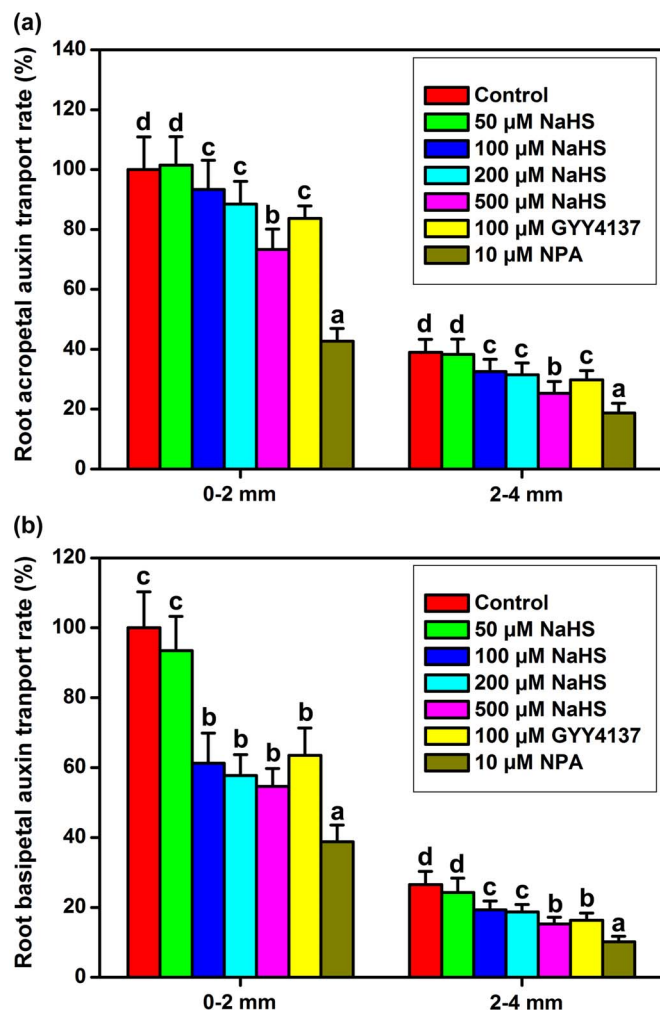


**Figure 4** | H<sub>2</sub>S regulates polar auxin transport in WT Arabidopsis root. Root acropetal auxin transport (a), and basipetal auxin transport (b) were assayed after various treatments for 12 h in 5-d-old seedlings. Mean values and SE are calculated from three replicates. Within each set of experiments, bars with different letters are significantly different ( $P < 0.05$ , Duncan's multiple range tests).

*PIN2* and *PIN7* decreased in 12 or 24 h (Fig. S3). The expression of *PIN4* decreased after treated with NaHS for 3 to 12 h, but recovered by 24 h (Fig. S3). However, the expression of *PIN3* did not show obvious changes after treatment with NaHS (Fig. S3). These experiments confirmed that H<sub>2</sub>S affects the localization of the PIN proteins.

#### The effects of H<sub>2</sub>S on F-actin and ABPs in the Arabidopsis root.

The actin cytoskeleton in eukaryotic cells is a highly organized and dynamic structure that plays a central role in numerous cellular processes, including intracellular transport, cell growth, and organelle positioning<sup>42</sup>. F-actin is known to affect the plasma membrane localization of PIN proteins, as the vesicle transport of PIN proteins depends on F-actin<sup>43,44</sup>. We examined the effects of H<sub>2</sub>S on the subcellular localization of F-actin (stained with fluorescein phalloidin), and the actin network in root epidermal cells observed by confocal microscopy. As shown in Fig. 6a, we observed that the elongation zone of the root tip and the actin network displayed thick, often longitudinally oriented cables and finer, randomly arranged filaments in the WT control. Treatment with NaHS or GYY4137 for 6 h caused significant changes in the actin cytoskeletal organization. After treatment, the thick actin cables were absent and the percentage of occupancy of F-actin bundles decreased in each cell (Fig. 6a).

A regulatory system that contains the actin filaments (F-actin) and actin-binding proteins (ABPs) is required for these processes, and the diverse actin cytoskeleton is directly controlled by different ABPs<sup>22,45,46</sup>. Actin depolymerizing factors (ADFs) sever F-actin and increase the rate of dissociation of actin monomers from the pointed ends<sup>47</sup>. Capping proteins (CPs) inhibit the growth of F-actin at the barbed end<sup>23</sup>. Profilins (PRFs) bind to G-actin to inhibit polymerization<sup>48</sup>. These proteins all have the potential to decrease the occupancy percentage of the F-actin bundles<sup>20,21,49</sup>. We examined the effects of H<sub>2</sub>S on the expression of *ADFs*, *CPs* and *PRFs*. qRT-PCR analysis showed that the expression of *ADF1* and *ADF4* decreased following NaHS treatment for 6 to 24 h (Fig. 7a), and the expression of *CPA*, *CPB* and *PRF3* increased after NaHS treatment in 3 to 24 h (Fig. 7b & c). We further examined the expression of *CPA::GUS*, *CPB::GUS* and *PRF3::GUS*. The results showed that the application of NaHS or GYY4137 significantly promoted *CPA::GUS* and *CPB::GUS* gene expression in the root apices (Fig. 8a). The *GUS* gene expression was also enhanced by NaHS in root and leaf samples of *PRF3::GUS* (Fig. 9a). The *GUS* activity showed a similar profile in the *CPA::GUS*, *CPB::GUS* and *PRF3::GUS* transgenic lines (Fig. 8b, c, & 9b). These data suggested that H<sub>2</sub>S may affect F-actin via regulating *CPA*, *CPB* and *PRF3* expression.

To validate this hypothesis, we observed the effects of H<sub>2</sub>S on F-actin in T-DNA insertion mutants *cpa* (*CP*  $\alpha$ -subunit (*CPA*) mutant), *cpb* (*CP*  $\beta$ -subunit (*CPA*) mutant) and *prf3*. As shown in Fig. 6, the percentage of occupancy of the F-actin bundles appeared to be somewhat more dense in the *cpa* and *cpb* cells than that in the WT cells. There were obvious differences in *cpa* and *cpb* compared with the WT cells after treatment with NaHS or GYY4137 for 3 to 12 h. The effects of NaHS and GYY4137 were partially removed in *cpa* and *cpb* (Fig. 6b). The *prf3* seedlings had similar amounts of F-actin bundles as the WT seedlings (Fig. 6b). However, the effects of NaHS and GYY4137 were also inhibited in the *prf3* seedlings compared with the WT seedlings in 3 to 12 h (Fig. 6b). These data imply that knock-out *CPA*, *CPB* or *PRF3* could partially remove the effects of H<sub>2</sub>S on the percentage of occupancy of the F-actin bundles.

#### The effects of H<sub>2</sub>S on auxin transport in the root of *cpa*, *cpb* and *prf3* mutant seedlings.

The acropetal and basipetal auxin transport rates were decreased in the *cpb* compared to the WT root samples (Fig. 10). In the roots of *cpa*, the basipetal auxin transport rates were decreased in 2 to 4 mm (Fig. 10). *prf3* displayed a similar auxin transport capacity as WT (Fig. 10). H<sub>2</sub>S could observably decrease the auxin transport rates in the WT sample (Fig. 4). Interestingly, there was an obvious difference between the mutant and WT plants after treatment with NaHS for 12 h. In the root of *cpb*, the effect of NaHS was removed in the acropetal auxin transport in both 0 to 2 mm and 2 to 4 mm, and in the basipetal auxin transport in 2 to 4 mm (Fig. 10). The weak auxin transport capacity was partially recovered compared with the WT levels in *cpa* and *prf3* after NaHS treatment for 12 h (Fig. 10). The H<sub>2</sub>S-induced inhibition of the primary root length was markedly removed in the *cpa*, *capb* and *prf3* mutant plants under 100  $\mu$ M NaHS treatment and partly removed in *capb* and *prf3* under 200  $\mu$ M NaHS (Fig. S4 and S5). These data suggest that *CPA*, *CPB* and *PRF3* play important roles in H<sub>2</sub>S by regulating auxin transport.

#### Discussion

The understanding of the importance of H<sub>2</sub>S as a regulator of plant growth and response to environmental stress has increased considerably despite the limited available information on its signaling. A physiological role for H<sub>2</sub>S in the regulation of root growth has been described<sup>30</sup>. H<sub>2</sub>S promotes adventitious root formation in batatas<sup>35</sup> and LR development in tomato plants<sup>36</sup>. Much of the work with H<sub>2</sub>S signaling has involved the pharmacological application of H<sub>2</sub>S donors such as NaHS to emulate H<sub>2</sub>S production<sup>15,50</sup>. Using different

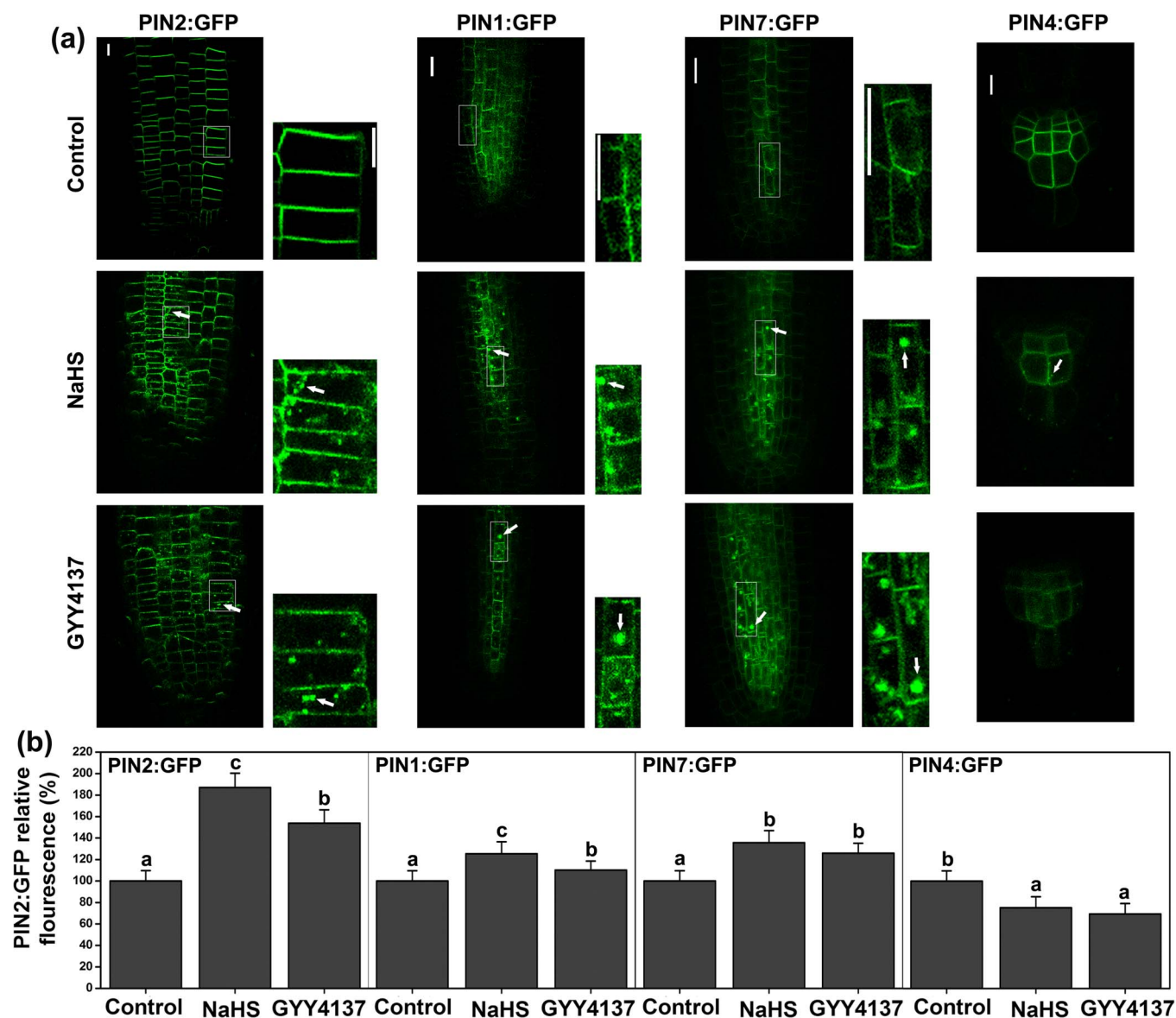


**Figure 5** |  $H_2S$  modulates the expression and distribution of PIN proteins in apical zone of the primary root. (a) Distribution of PIN1:GFP, PIN2:GFP, PIN4:GFP and PIN7:GFP proteins were shown in untreated control plants, treated with 200  $\mu M$  NaHS and treated with 100  $\mu M$  GYY4137 for 6 h. Images shown are representative of each treatment. Scale bar = 5  $\mu m$ . (b) Fluorescence density of PIN1:GFP, PIN2:GFP, PIN4:GFP and PIN7:GFP, the transgenic lines were treated with NaHS or GYY4137 for 6 h. Data are mean values and SE ( $n > 25$ ) in (a) and (b). The arrows indicated the compartments formation of PINs. Within each set of experiments, bars with different letters are significantly different ( $P < 0.05$ , Duncan's multiple range tests).

$H_2S$  donors (NaHS and GYY4137), we confirmed that increased endogenous  $H_2S$  levels inhibited primary root and root hair growth but promoted LR formation in *Arabidopsis* (Fig. 1, Fig. S1 & S2). However, the mechanisms of the precise cellular responses to  $H_2S$  are not yet well understood. Therefore, the discovery of the novel signaling molecule  $H_2S$ , which is involved in triggering root system architecture, was an important outcome of this work.

The process of root organogenesis is controlled by auxin<sup>51</sup>. Previous studies have demonstrated that  $H_2S$  interacts with auxin in modulating root system growth<sup>35,36</sup>. Using *DR5::GUS*, an indirect indicator of the level and distribution of auxin, we observed that high concentrations of endogenous  $H_2S$  attenuate auxin-dependent reporter expression in the QC and in the three layers of the columella cells (Fig. 3a). The maximum auxin distribution is found in the root apex, which is necessary for meristem maintenance<sup>52</sup>. The maximum levels are normally observed in the QC, columella initial cells and

mature columella cells of the root apices, but this maximum is diminished by the presence of elevated  $H_2S$  cells in the primary root apex (Fig. 3a). Additionally, we used [ $^3H$ ]-IAA to measure auxin transport directly. When endogenous  $H_2S$  levels are increased by NaHS or GYY4137, the IAA movement is reduced in the root (Fig. 4). Moreover, the application of the low concentration auxin (5 nM IAA) partially removed the effects of NaHS (Fig. S6). Taken together, the evidence supports the hypothesis that  $H_2S$  perturbs auxin distribution and transport in the root apical meristem, which inhibits the primary root elongation.

LR development is initiated by asymmetric divisions in pairs of founder cells within xylem pole pericycle cells. When the auxin levels reach a certain threshold, which is sensed and transduced by the xylem pole pericycle cells, the cell cycle machinery becomes activated, resulting in progression to the S phase<sup>3</sup>. Thus, the auxin maximum is required for LRP initiation<sup>39</sup>. Although  $H_2S$  changes the

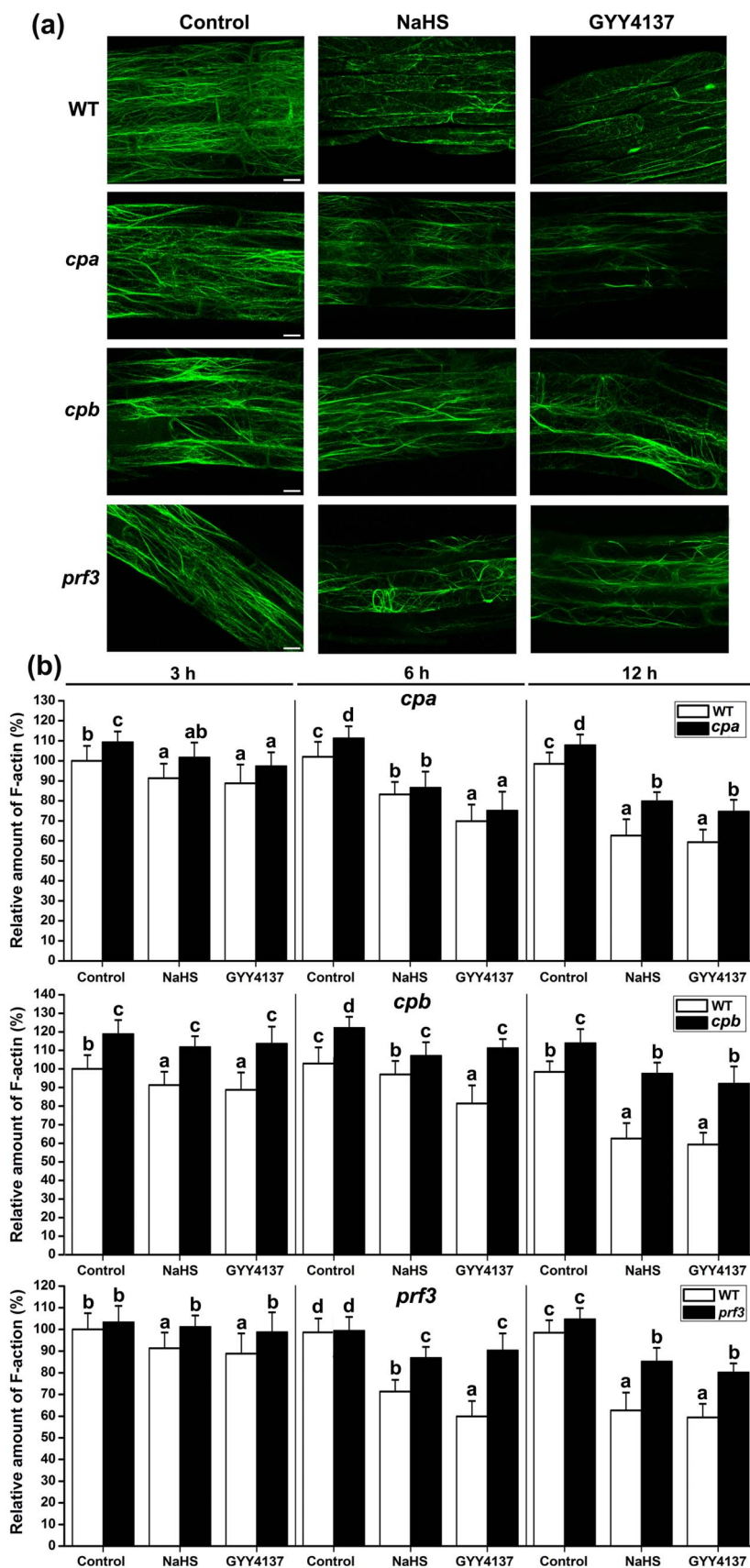


**Figure 6** | Effects of H<sub>2</sub>S on F-actin in root of WT, *cpa*, *cpb* and *prf3*. (a) Distribution of F-actin was shown in untreated control plants, treated with 200 μM NaHS or with 100 μM GYY4137 for 6 h. Images shown are representative of each treatment. Scale bar = 10 μm. (b) Quantification of the relative F-actin levels. The amount of F-actin in untreated WT roots was normalized to 100% as the control. Data are mean values and SE (n > 25) in (a) and (b). Within each set of experiments, bars with different letters are significantly different (P < 0.05, Duncan's multiple range tests).



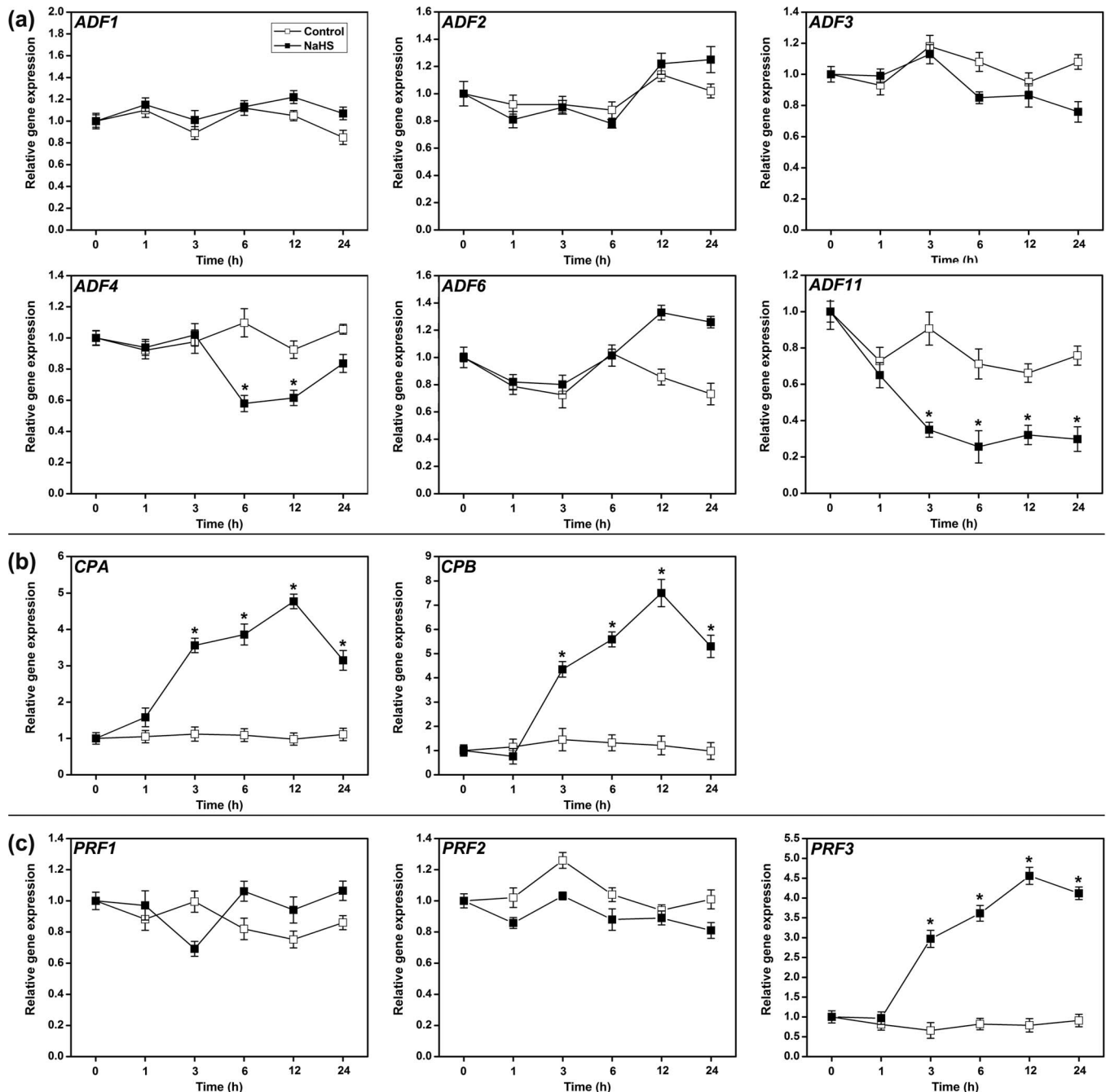


**Figure 7** | qRT-PCR analysis of ABPs genes in WT Arabidopsis root. Relative expression levels are normalized with an internal standard *EF1a*. 5-d-old Arabidopsis WT seedlings were grown on agar plates supplied with 200  $\mu$ M NaHS for 1–24 h. Mean values and SE are calculated from three replicates. Within each set of experiments, bars with different letters are significantly different ( $P < 0.05$ , Duncan's multiple range tests).

auxin maximum distribution in the primary root apices,  $H_2S$  does not alter the auxin maximum distribution in the entire stage of LRP development (stages I–VII) (Fig. 3d). In addition, the application of the  $H_2S$  donor increased the density of LRP and LR (Fig. 2b & c), indicating that auxin transport may play an important role in the  $H_2S$ -induced LR formation.

Plants can transfer IAA from source tissues to the root and shoot apices and other sink tissues, and this depends on the differential auxin transport components<sup>7</sup>. The PIN proteins are required for auxin transport; the PIN2 protein is a key regulator of basipetal IAA movement and the PIN1 protein regulates the acropetal IAA movement. Both PIN1 and PIN2 are important for root architecture development<sup>39</sup>. In the PIN family, PIN1, 3, 4 and 7 regulate LR

formation<sup>39</sup>. The *pin1* mutant and the *pin3pin4pin7* triple mutant show strongly reduced bending of the LRs<sup>14,51</sup>. Except for *PIN3* and *PIN4*, the expression of *PIN1*, *PIN2* and *PIN7* were enhanced when the endogenous  $H_2S$  level increased (Fig. S3). However, the IAA transport capacity was inhibited by  $H_2S$ , suggesting that the gene expression of PIN proteins may not be a key factor in the  $H_2S$  regulation of auxin transport. The polar subcellular distribution of the PIN proteins at the plasma membrane determines the function of the PIN proteins<sup>40</sup>. We followed the localization of the fluorescent markers with different polar localization in the epidermal cells: the polar distribution of PIN1:GFP, PIN2:GFP, PIN4:GFP and PIN7:GFP were altered by  $H_2S$  by changing the vesicle transport of the PIN proteins. In addition,  $H_2S$  signaling delayed the recycling of PIN

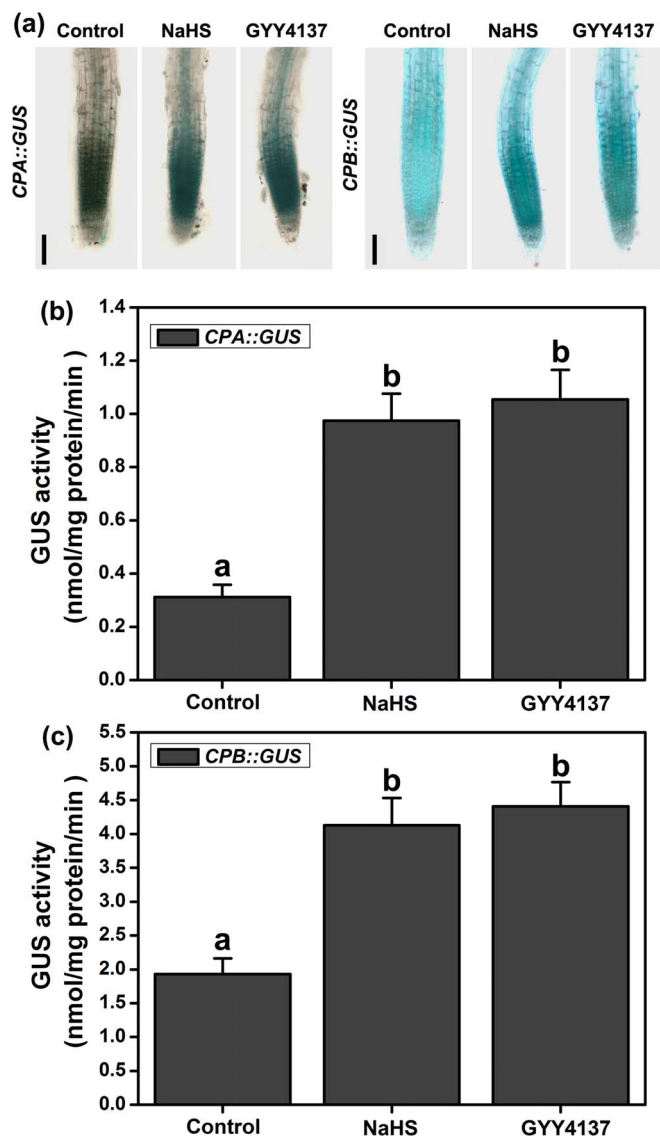


**Figure 8** | Effects of  $H_2S$  on the expression of *CPA::GUS* and *CPB::GUS* in the roots of the transgenic lines. (a) Histochemical GUS staining patterns of *CPA::GUS* and *CPB::GUS* in 5-d-old seedlings treated with 200  $\mu M$  NaHS or 100  $\mu M$  GYY4137 for 6 h. Images shown are representative of each treatment. Scale bar = 100  $\mu m$ . (b) GUS activity of *CPA::GUS* and *CPB::GUS* in the roots of 5-d-old seedlings treated with 200  $\mu M$  NaHS or 100  $\mu M$  GYY4137 for 6 h. Data are mean values and SE ( $n > 25$ ) in (a). Mean values and SE are calculated from three replicates in (b) and (c). Within each set of experiments, bars with different letters are significantly different ( $P < 0.05$ , Duncan's multiple range tests).

proteins between the endomembrane compartments and the PM (Fig. S8). These results reveal that the loss of polar PIN protein localization results in the  $H_2S$ -induced decrease in the auxin transport capacity.

Vesicle trafficking of PIN proteins is an actin-dependent process<sup>41</sup>. The actin cytoskeleton regulates many physiological processes and controls endocytosis, exocytosis, and vesicle trafficking. Actin-dependent vesicle trafficking is also affected by signaling molecules<sup>53</sup>. Increases in the  $H_2S$  levels could decrease the occupancy of F-actin bundles in root epidermic cells (Fig. 6a). In conclusion, we have demonstrated for the first time that  $H_2S$  has the capacity to affect the percentage of F-actin. Thus, we speculate that F-actin may act as a downstream effector of  $H_2S$  signaling and may thus affect the vesicle trafficking of PIN proteins. We further predict that it is a key regu-

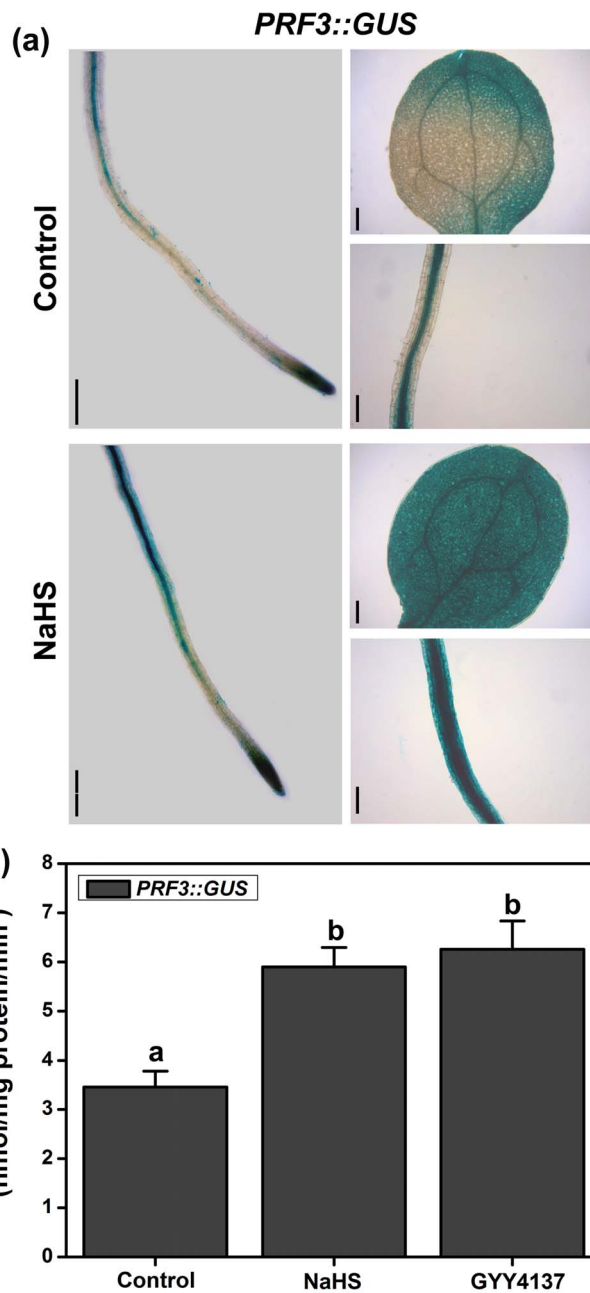


**Figure 9** | Effects of  $H_2S$  on the expression of *PRF3::GUS* in the transgenic lines. (a) Histochemical GUS staining patterns of *PRF3::GUS* in 5-d-old seedlings treated with 200  $\mu M$  NaHS for 6 h. Images shown are representative of each treatment. Scale bar = 200  $\mu m$ . (b) GUS activity of *PRF3::GUS* in the root of 5-d-old seedlings treated with 200  $\mu M$  NaHS or 100  $\mu M$  GYY4137 for 6 h. Data are mean values and SE ( $n > 25$ ) in (c). Mean values and SE are calculated from three replicates in (b). Within each set of experiments, bars with different letters are significantly different ( $P < 0.05$ , Duncan's multiple range tests).

lator of cellular responses to  $H_2S$  signaling. However, signaling-induced reorganizations or changes in the actin cytoskeleton often require ABPs as the stimulus response modulators<sup>24</sup>. Alternatively,  $H_2S$  might therefore directly affect F-actin or some of the ABPs. Here, qRT-PCR analysis showed that the transcription of some of the ABPs (including *CPA*, *CPB* and *PRF3*) increased after treatment of  $H_2S$  donor for a short time (Fig. 7b & c). GUS activities were also enhanced in the *CPA::GUS*, *CPB::GUS* and *PRF3::GUS* transgenic lines following  $H_2S$  treatment (Fig. 8 & 9). In addition, the effects of

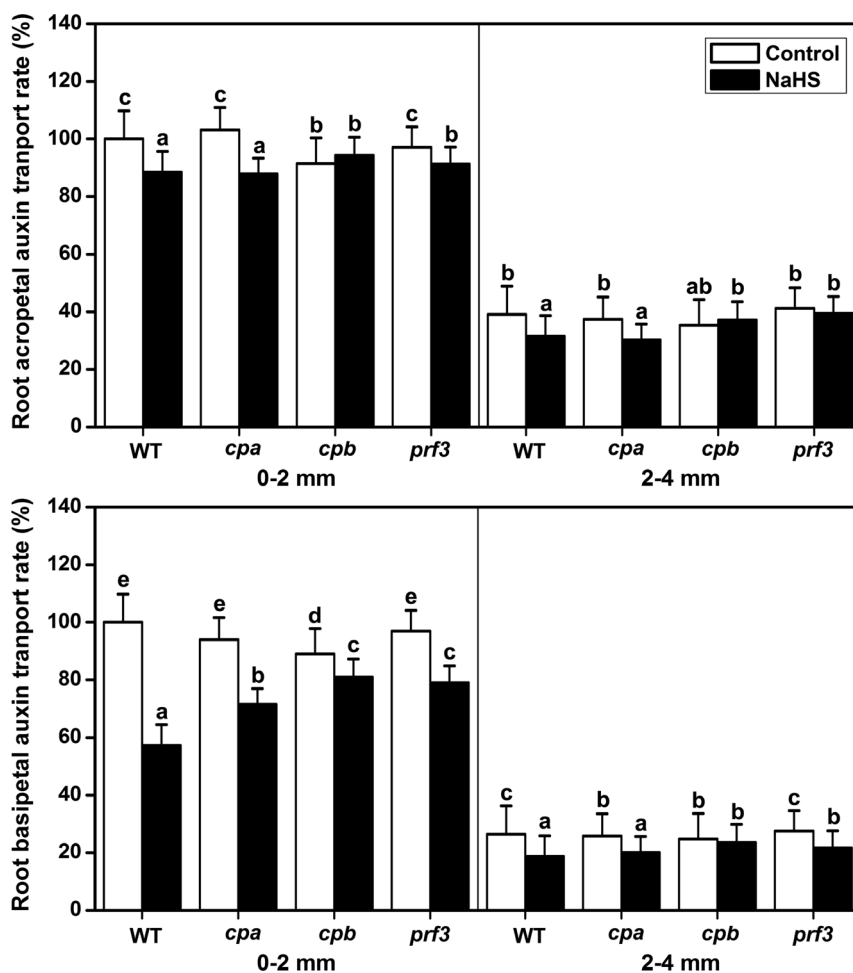


**Figure 10** | H<sub>2</sub>S modulates polar auxin transport in root of WT, *cpa*, *cpb* and *prf3*. Root acropetal auxin transport (a), and basipetal auxin transport (b) were assayed after NaHS treatments for 12 h in 5-d-old seedlings. Mean values and SE are calculated from three replicates. Within each set of experiments, bars with different letters are significantly different ( $P < 0.05$ , Duncan's multiple range tests).

H<sub>2</sub>S on PIN2 immunolocalization were partially weakened in the *cpb* mutants (Fig. 7S). Taken together, these data imply that H<sub>2</sub>S might primarily affect ABPs and then alter the morphology of actin cytoskeleton, therefore acting as the secondary effect response to H<sub>2</sub>S exposure. To confirm this hypothesis, we observed the effects of H<sub>2</sub>S on F-actin in T-DNA insertion mutants of *cpa*, *cpb* and *prf3*. Our observations indicated that the effects of H<sub>2</sub>S on F-actin were partially removed in the *cpa*, *cpb* and *prf3* mutant plants (Fig. 6). This finding suggests that H<sub>2</sub>S effectively regulates several ABPs, which are critical for the assembly and depolymerization of F-actin. Interestingly, the inhibitory role of H<sub>2</sub>S on auxin transport was also partially recovered compared to the WT plants in the *cpa*, *cpb* and *prf3* mutant plants (Fig. 10), suggesting that several ABPs can act as the direct regulator responses to H<sub>2</sub>S signaling on actin-dependent auxin transport.

In conclusion, our results provide a new insight into how H<sub>2</sub>S triggers changes in auxin transport and distribution in Arabidopsis roots. In the present study, we have provided evidence that high levels of H<sub>2</sub>S will inhibit auxin distribution and transport and will lead to alterations of root system development, including alterations in the primary root, LP and root hair. Our study suggests that the H<sub>2</sub>S-inhibited auxin transport in the Arabidopsis roots is due to alterations in the assembly and depolymerization of F-actin. In this process, the ABPs act as downstream effectors of H<sub>2</sub>S signal transduction, which regulate depolymerization of F-actin in the root cells. Finally, the distribution and transport of auxin are altered. To our knowledge, this is the first molecular evidence that H<sub>2</sub>S signaling

regulates the remodeling of root system architecture by affecting auxin transport and actin cytoskeleton development in Arabidopsis. The regulative mechanism of H<sub>2</sub>S signaling on plant growth is very complicated. Our data suggest the existence of a tightly regulated intertwined signaling network between auxin, H<sub>2</sub>S and ABPs that is responsible for controlling root system development. Auxin can also affect the patterning and organization of the actin cytoskeleton during cell growth<sup>6,54</sup>. On the other hand, the actin cytoskeleton partially affects the directional transport of auxin by modulating the cycling of auxin efflux carriers<sup>44,55</sup>. The effects of H<sub>2</sub>S on root growth occur through a complex process. Alterations in the distribution may further affect its own transport and actin cytoskeleton. Thus, further research is required for the elucidation of the detailed molecular mechanisms involved in H<sub>2</sub>S-induced auxin homeostasis changes in plants.

## Methods

**Plant material and chemical treatments.** This study was carried out on *Arabidopsis thaliana* including WT ecotypes Columbia (Col-0), the transgenic lines PIN1::GFP, PIN2::GFP, PIN4::GFP, PIN7::GFP, DR5::GUS, CPA::GUS, CPB::GUS, PRF3::GUS and the *cpa*, *cpb* and *prf3* mutants. Seeds were surface sterilized with 70% ethanol for 30 s and 15% sodium hypochlorite for 15 min, and washed five times with sterilized water before sowing on solid 1/2 Murashige and Skoog (MS) medium (pH 5.7) containing 1% (w/v) sucrose, 0.8% (w/v) agar. After that, the seeds were vernalized for 2 d at 4°C. Then the seedlings were grown in a growth room, which has the temperature at 22 ± 1°C and with a 14/10 h light/dark photoperiod under a photon flux density of 120 μmol m<sup>-2</sup>s<sup>-1</sup>. The Arabidopsis plants used throughout this work were grown routinely in a growth chamber under 50–60% humidity.



Following 3 or 5 d growth, Arabidopsis seedlings were transferred to the 1/2 MS agar medium. 50–1000  $\mu\text{M}$  sodium hydrosulfide (NaHS), 100  $\mu\text{M}$  p-(methoxyphenyl) morpholino-phosphino-dithioic acid (GY4137), 10  $\mu\text{M}$  N-1-naphthylphthalamic acid (NPA) were added to the medium for various treatments. The  $\text{H}_2\text{S}$  donors NaHS and GY4137, and NPA were purchased from Sigma.

**Measurement of  $\text{H}_2\text{S}$  content.** Hydrogen sulfide quantification was performed as described by Nashef<sup>56</sup>. Briefly, the root of seedlings were ground into fine powder with a mortar and pestle under liquid nitrogen and 0.3 g of frozen tissue were homogenized in 1 ml of 100 mM potassium phosphate buffer (pH 7.0) containing 10 mM EDTA. The homogenate was centrifuged at 15,000 g for 20 min at 4°C and 100  $\mu\text{l}$  of the supernatant was used for the quantification of  $\text{H}_2\text{S}$ , in an assay mixture containing also 1880  $\mu\text{l}$  extraction buffer and 20  $\mu\text{l}$  of 20 mM 5,5'-dithiobis (2-nitrobenzoic acid), in a total volume of 2 ml. The assay mixture was incubated at room temperature for 2 min and the absorbance was read at 412 nm. Hydrogen sulfide was quantified based on a standard curve of known concentrations of NaHS.

**Morphology measurements.** After transferring the 3-d-old seedlings to various treatments for 2 or 4 d, we analyzed the number of primary roots, the LRP and the LR with a dissecting microscope. At least 25 roots were analyzed per replicate. The number of LRs (longer than 0.5 mm in the length of LR) was counted. LRPs were classified and counted according to their stage of development using the methods and nomenclature described in Malamy and Benfey<sup>39</sup>. LRs that had emerged but were shorter than 0.5 mm were classified as LRPs, and the density of LRPs was determined by counting the number per seedling. For each treatment, at least 25 seedlings were used for the morphology measurements. These experiments were repeated three times. Root hairs were photographed with an Olympus stereo microscope and the number of root hairs was counted in a 2 mm region from the primary root apex. The length of the primary roots, LRs and root hairs were measured with NIH Image software (Image J, version 1.43).

**Confocal microscopy and fluorescence intensity analysis.** We used PIN1:GFP, PIN2:GFP, PIN4:GFP and PIN7:GFP to analyze the localizations of PIN1, PIN2, PIN4 and PIN7 in Arabidopsis ecotype Columbia (Col-0). The 5-d-old seedlings were used to observe the subcellular localization. For the various chemical treatments, 5-d-old seedlings were transferred to the 1/2 MS agar medium, which contained different chemicals, and were treated for 6 h. Fluorescent images were obtained using the Olympus DP72 laser confocal scanning microscope. For the GFP fluorescence observations, we used argon laser excitation at 488 nm with a 505–550 nm emission filter set. The anti-PIN1 antibody and the anti-PIN2 antibody from Sigma-Aldrich were diluted by 1:300. Secondary antibodies were diluted by 1:1000. To obtain the shown views, we scanned for another 2.5  $\mu\text{m}$  after seeing the PIN-GFP proteins; thickness of every slice was 0.5  $\mu\text{m}$ . Image J software was used to analyze the green fluorescence intensity.

**Actin Staining of root and confocal microscopy observation.** To analyze the dynamic F-actin networks, F-actin was stained as previously described with slight modifications<sup>57</sup>. 5-d-old seedlings isolated from the WT and mutant plants were prefixed for 20 min in 1% stationary liquid, which was freshly prepared from 1% paraformaldehyde and 0.025% glutaraldehyde in PME buffer (100 mM PIPES, 5 mM  $\text{MgSO}_4$ , 10 mM EGTA, pH 6.8). Then, the seedlings were immersed in 2% paraformaldehyde and 0.05% glutaraldehyde in PME for 20 min. Finally, the seedlings were fixed in a final concentration of 4% paraformaldehyde and 0.1% glutaraldehyde in PME for 20 min. After three washes in PME, the seedlings were stained using 0.3  $\mu\text{M}$  Alexa 488-phalloidin (Molecular Probes) diluted in PME buffer with 5% dimethyl sulfoxide and 0.05% NP-40 overnight in the dark. Fluorescent images were captured using a confocal laser scanning microscope (Olympus DP72) equipped with a 40 $\times$  objective. The GFP fluorescence images were collected using a 488 nm excitation laser line and a 505–530 nm band pass emission filter. To measure the amount of F-actin in the root cells, the images were captured under the same conditions. All images were analyzed using Image J software and the amount of F-actin was calculated by measuring the pixel intensity of the individual cells<sup>58</sup>.

**Histochemical analyses.** GUS activity analysis employed a histochemical assay, which was performed as described with minor modifications<sup>59</sup>. Histochemical analysis was completed in 5-d-old DR5::GUS, CPA::GUS, CPB::GUS and PRF3::GUS seedlings. Seedlings were transferred to 1/2 MS agar medium containing different chemicals and treated for 6 h. Then, the samples were collected and used for the following assays. Seedlings were incubated in GUS-staining buffer containing 1 mM X-Gluc, 0.5 mM potassium ferricyanide, 100 mM sodium phosphate (pH 7.5), 0.5 mM potassium ferrocyanide, 10 mM EDTA and 0.1% Triton X-100. Tissues were incubated at 37°C for 6 h and then fixed with 70% (v/v) ethanol ( $n \geq 25$ ). Samples were photographed with the dissecting microscope.

**Quantitative GUS activity assay.** The substrate 4-methylumbelliferyl- $\beta$ -D-glucuronide (MUG) (Sigma) was used to assay the GUS activity<sup>59</sup>. Roots of the seedlings were frozen in liquid nitrogen and ground in a 300  $\mu\text{l}$  MUG extraction buffer composed of sodium phosphate (50 mM, pH 7.0), 10 mM EDTA (pH 8.0), 10 mM  $\beta$ -mercaptoethanol, 0.1% (v/v) Triton X-100 and 0.1% (w/v) N-lauroyl sarcosine (SLS) (Sigma). The extract was spun, and the supernatant was extracted. 10  $\mu\text{l}$  of the extract was mixed with 390  $\mu\text{l}$  of the GUS assay buffer and incubated at 37°C for 1 h. The samples were stopped with 0.2 M  $\text{Na}_2\text{CO}_3$ . Fluorescence was

determined by DyNA Quant 200. The protein concentration was measured according to Peterson's<sup>60</sup> modification of the Lowry method. Approximately 40 seedlings were subjected to each treatment.

**Auxin transport assays.** Acropetal auxin transport was measured in the root system, as described by Buer and Muday<sup>61</sup>, while Basipetal auxin transport was measured in the root system, as described by Shin<sup>13</sup>. The following modifications were applied to these methods. Here, 1 mm diameter agar blocks containing  $7.76 \times 10^8$  M [ $^3\text{H}$ ]-IAA (PerkinElmer, USA) were applied to the root-shoot transition zone. After treatment with NaHS, GY4137 and NPA for 24 h, a 0.5 mm section of the root close to the agar block was dissected and discarded. 2 mm consecutive segments below the incision line were then collected separately and pooled from 6 to 10 roots and placed in glass scintillation vials containing 5 ml scintillation solution. A Beckman Coulter LS6500 Scintillation Counter (Fullerton, CA, USA) was used to measure the radioactivity in these two pools of root segments. The radioactivity values are reported as means  $\pm$  standard deviation from three independent experiments. The observed effects were corroborated by a NPA block assay<sup>4</sup>.

**RNA isolation and qRT-PCR.** Roots of Col-0 were harvested to extract total RNA for real-time PCR. Total RNA was extracted using RNeasy pure plant kit (Qiagen, Beijing) and treated with RNase free DNase (Qiagen). The total RNA was reverse-transcribed into first-strand cDNA using PrimeScript<sup>TM</sup> Reverse Transcriptase (Takara, Japan) and Oligo (dT)<sub>15</sub> primer (Takara) following the manufacturer's instructions. The samples were amplified using SYBR Green I (SYBR<sup>®</sup> Premix Ex Taq<sup>TM</sup> Kit, Takara). The housekeeping gene *EF1A* was used as an internal control. The thermal cycle used was as follows: 95°C for 10 s, and 40 cycles of 95°C for 5 s and 59°C for 25 s. This was followed by 80 cycles of 10 s during the time elapsed during 55–95°C. The PCR amplifications for each gene were performed in triplicate. The results were analyzed by Rotor-Gene Real-Time Analysis Software 6.1 (Build 81). All the primers used in this study were shown in Table S1.

**Statistical analysis.** Each experiment was repeated at least three times and three replications in each time. Values were expressed as means  $\pm$  SE. For all experiments, the overall data were statistically analyzed in the SPSS version 17.0 (SPSS). Duncan's multiple range tests were used. The statistical analysis of two groups was performed using Student's *t*-test. In all cases, the confidence coefficient was set at 0.05.

- Woodward, A. W. & Bartel, B. Auxin: regulation, action, and interaction. *Ann. Bot.-London* **95**, 707–35 (2005).
- Normanly, J. Approaching cellular and molecular resolution of auxin biosynthesis and metabolism. *Cold Spring Harbor Perspectives in Biology* **2**, 001594–001601 (2010).
- Benková, E. *et al.* Local, efflux-dependent auxin gradients as a common module for plant organ formation. *Cell* **115**, 591–602 (2003).
- Rashotte, A. M., Brady, S. R., Reed, R. C., Ante, S. J. & Muday, G. K. Basipetal auxin transport is required for gravitropism in roots of Arabidopsis. *Plant Physiol.* **122**, 481–490 (2000).
- Dubrovsky, J. G. *et al.* Auxin minimum defines a developmental window for lateral root initiation. *New Phytol.* **191**, 970–983 (2011).
- Rahman, A. *et al.* Auxin, actin and growth of the Arabidopsis thaliana primary root. *Plant J.* **50**, 514–528 (2007).
- Vanneste, S. & Friml, J. Auxin: a trigger for change in plant development. *Cell* **136**, 1005–1016 (2009).
- Kleine-Vehn, J., Dhonukshe, P., Swarup, R., Bennett, M. & Friml, J. Subcellular trafficking of the Arabidopsis auxin influx carrier AUX1 uses a novel pathway distinct from PIN1. *Plant Cell* **18**, 3171–3181 (2006).
- Yang, Y., Hammes, U. Z., Taylor, C. G. & Schachtman, D. P. Nielsen E high-affinity auxin transport by the AUX1 influx carrier protein. *Curr. Biol.* **6**, 1123–1127 (2006).
- Santelia, D. *et al.* MDR-like ABC transporter AtPGP4 is involved in auxin-mediated lateral root and root hair development. *FEBS Lett.* **579**, 5399–5406 (2005).
- Friml, J. *et al.* Efflux-dependent auxin gradients establish the apical-basal axis of Arabidopsis. *Nature* **426**, 147–153 (2003).
- Bilou, I. *et al.* The PIN auxin efflux facilitator network controls growth and patterning in Arabidopsis roots. *Nature* **433**, 39–44 (2005).
- Shin, H. *et al.* Complex regulation of Arabidopsis AGR1/PIN2-mediated root gravitropic response and basipetal auxin transport by cantharidin-sensitive protein phosphatases. *Plant J.* **42**, 188–200 (2005).
- Rosquete, M. R. *et al.* An auxin transport mechanism restricts positive orthogravitropism in lateral roots. *Curr. Biol.* **23**, 817–822 (2013).
- Li, J. S. & Jia, H. L. cGMP modulates Arabidopsis lateral root formation through regulation of polar auxin transport. *Plant Physiol. & Biochem.* **66**, 105–117 (2013).
- Dubrovsky, J. G. *et al.* Auxin acts as a local morphogenetic trigger to specify lateral root founder cells. *Proc. Natl. Acad. Sci. USA* **105**, 8790–8794 (2008).
- Geldner, N. *et al.* Partial loss-of-function alleles reveal a role for GNOM in auxin transport-related, post-embryonic development of Arabidopsis. *Development* **131**, 389–400 (2004).
- Hussey, P. J., Ketelaar, T. & Deeks, M. J. Control of the actin cytoskeleton in plant cell growth. *Annu. Rev. Plant Biol.* **57**, 109–125 (2006).



19. Kandasamy, M. K., McKinney, E. C. & Meaghe, R. B. A single vegetative actin isovariant overexpressed under the control of multiple regulatory sequences is sufficient for normal Arabidopsis development. *Plant Cell* **21**, 701–718 (2009).
20. Fan, T. *et al.* Overexpression of profilin 3 affects cell elongation and F-actin organization in *Arabidopsis thaliana*. *Plant Cell Rep.* **32**, 149–160 (2013).
21. Li, L., Wang, Y. & Shen, W. Roles of hydrogen sulfide and nitric oxide in the alleviation of cadmium-induced oxidative damage in alfalfa seedling roots. *Biometals* **25**, 617–631 (2012).
22. Jia, H. *et al.* Arabidopsis CROLIN1, a novel plant actin-binding protein, functions in cross-linking and stabilizing actin filaments. *J. Biol. Chem.* **288**, 32277–32288 (2013).
23. Huang, S., Blanchoin, L., Kovar, D. R. & Staiger, C. J. Arabidopsis capping protein (AtCP) is a heterodimer that regulates assembly at the barbed ends of actin filaments. *J. Bio. Chem.* **278**, 44832–44842 (2003).
24. Huang, S., Gao, L., Blanchoin, L. & Staiger, C. J. Heterodimeric capping protein from Arabidopsis is regulated by phosphatidic acid. *Mol. Bio. Cell* **17**, 1946–1958 (2006).
25. Nagai, Y., Tsugane, M., Oka, J. & Kimura, H. Hydrogen sulfide induces calcium waves in astrocytes. *FASEB J.* **18**, 557–559 (2004).
26. García-Mata, C. & Lamattina, L. Hydrogen sulfide, a novel gasotransmitter involved in guard cell signalling. *New Phytol.* **188**, 977–984 (2010).
27. Tan, B. H., Wong, P. T. H. & Bian, J. S. Hydrogen sulfide: a novel signaling molecule in the central nervous system. *Neurochem. Int.* **56**, 3–10 (2010).
28. Wilson, L. G., Bressan, R. A. & Filner, P. Light-dependent emission of hydrogen sulfide from plants. *Plant Physiol.* **61**, 184–189 (1978).
29. Christou, A., Manganaris, G. A., Papadopoulos, I. & Fotopoulos, V. Hydrogen sulfide induces systemic tolerance to salinity and non-ionic osmotic stress in strawberry plants through modification of reactive species biosynthesis and transcriptional regulation of multiple defence pathways. *J. Exp. Bot.* **647**, 1953–1966 (2013).
30. Li, J. S., Jia, H. L., Wang, J., Cao, Q. & Wen, Z. Hydrogen sulfide is involved in maintaining ion homeostasis via regulating plasma membrane Na<sup>+</sup>/H<sup>+</sup> antiporter system in the hydrogen peroxide-dependent manner in salt-stress *Arabidopsis thaliana* root. *Protoplasma* **251**, 899–912 (2014).
31. Li, Z. G., Yang, S. Z., Long, W. B., Yang, G. X. & Shen, Z. Z. Hydrogen sulfide may be a novel downstream signal molecule in nitric oxide-induced heat tolerance of maize (*Zea mays* L.) seedlings. *Plant Cell and Environ.* **36**, 1564–1572 (2013).
32. Chen, J. *et al.* Hydrogen sulfide alleviates aluminum toxicity in barley seedlings. *Plant Soil* **362**, 301–318 (2013).
33. Zhang, H. *et al.* Hydrogen sulfide promotes wheat seed germination and alleviates the oxidative damage against copper stress. *J. Integr. Plant Biol.* **50**, 1518–1529 (2008).
34. Dooley, F. D., Nair, S. P. & Ward, P. D. Increased growth and germination success in plants following hydrogen sulfide administration. *Plos one* **8**, 62048–62052 (2013).
35. Zhang, H. *et al.* Hydrogen Sulfide Promotes Root Organogenesis in *Ipomoea batatas*, *Salix matsudana* and *Glycine max*. *J. Integr. Plant Biol.* **51**, 1086–1094 (2009).
36. Fang, T., Cao, Z., Lia, Z., Shen, W. & Huang, L. Auxin-induced hydrogen sulfide generation is involved in lateral root formation in tomato. *Plant Physiol. & Biochem.* **76**, 44–51 (2014).
37. Fernández-Marcos, M., Sanz, L., Lewis, D. R., Muday, G. K. & Lorenzo, O. Nitric oxide causes root apical meristem defects and growth inhibition while reducing PIN-FORMED 1 (PIN1)-dependent acropetal auxin transport. *Proc. Natl. Acad. Sci. USA* **108**, 18506–18511 (2011).
38. Malamy, J. E. & Benfey, P. N. Organization and cell differentiation in lateral roots of *Arabidopsis thaliana*. *Development* **124**, 33–44 (1997).
39. Péret, B. *et al.* Arabidopsis lateral root development: an emerging story. *Trends Plant Sci.* **14**, 399–408 (2009).
40. Wiśniewska, J. *et al.* Polar PIN localization directs auxin flow in plants. *Science* **312**, 883 (2006).
41. Grunewald, W. & Friml, J. The march of the PINs: Developmental plasticity by dynamic polar targeting in plant cells. *EMBO J.* **29**, 2700–2714 (2010).
42. Staiger, C. J. Signaling to the actin cytoskeleton in plants. *Annual Review of Plant Physiology and Plant Mol. Biol.* **51**, 257–288 (2000).
43. Dhonukshe, P. *et al.* Auxin transport inhibitors impair vesicle motility and actin cytoskeleton dynamics in diverse eukaryotes. *Proc. Natl. Acad. Sci. USA* **105**, 4489–4494 (2008).
44. Mudaya, G. K. & Murphy, A. S. An emerging model of auxin transport regulation. *Plant Cell* **14**, 293–299 (2002).
45. Meagher, R. B. & Williamson, R. E. The plant cytoskeleton. In *Arabidopsis*, Meyerowitz E, Somerville C, eds. *Cold Spring Harbor Laboratory*, Cold Spring Harbor, NY, pp 1049–1084 (1994).
46. Pollard, T. D. & Cooper, J. A. Actin, a central player in cell shape and movement. *Science* **326**, 1208–1212 (2009).
47. Pavlov, D., Muhrad, A., Cooper, J., Wear, M. & Reisler, E. Actin filament severing by cofilin. *J. Mol. Biol.* **365**, 1350–1358 (2007).
48. Finkel, T., Theriot, J. A., Dise, K. R., Tomaselli, G. F. & Goldschmidt-Clermont, P. J. Dynamic actin structures stabilized by profilins. *Proc. Natl. Acad. Sci. USA* **91**, 1510–1514 (1994).
49. Wang, J. *et al.* Arabidopsis actin capping protein (AtCP) subunits have different expression patterns, and downregulation of AtCPB confers increased thermotolerance of Arabidopsis after heat shock stress. *Plant Sci.* **193–194**, 110–119 (2012).
50. Wang, Y. *et al.* Hydrogen sulfide enhances alfalfa (*Medicago sativa*) tolerance against salinity during seed germination by nitric oxide pathway. *Plant Soil* **351**, 107–119 (2012).
51. Sabatini, S. *et al.* An auxin-dependent distal organizer of pattern and polarity in the Arabidopsis root. *Cell* **99**, 463–472 (1999).
52. Petersson, S. V. *et al.* An auxin gradient and maximum in the Arabidopsis root apex shown by high-resolution cell-specific analysis of IAA distribution and synthesis. *Plant Cell* **21**, 1659–1668 (2009).
53. Kasprzewicz, A., Szuba, A., Volkmann, D., Baluška, F. & Wojtaszek, P. Nitric oxide modulates dynamic actin cytoskeleton and vesicle trafficking in a cell type-specific manner in root apices. *J. Exp. Bot.* **60**, 1605–1617 (2009).
54. Lanza, M. *et al.* Role of actin cytoskeleton in brassinosteroid signaling and in its integration with the auxin response in plants. *Dev. Cell* **22**, 1275–1285 (2012).
55. Sun, H., Basu, S., Brady, S. R., Luciano, R. L. & Muday, G. K. Interactions between auxin transport and the actin cytoskeleton in developmental polarity of *Fucus distichus* embryos in response to light and gravity. *Plant Physiol.* **135**, 266–278 (2004).
56. Nashef, A. S., Osuga, D. T. & Feeney, R. E. Determination of hydrogen sulfide with 5,5 β'-dithiobis-(2-nitrobenzoic acid), N-ethylmaleimide, and parachloromercuribenzoate. *Analytical Biochem.* **79**, 394–405 (1977).
57. Nishimura, T., Yokota, E., Wada, T., Shimmen, T. & Okada, K. An Arabidopsis ACT2 dominant-negative mutation, which disturbs F-actin polymerization, reveals its distinctive function in root development. *Plant Cell Physiol.* **44**, 1131–1140 (2003).
58. Zhang, H. *et al.* Arabidopsis VILLIN5, an actin filament bundling and severing protein, is necessary for normal pollen tube growth. *Plant Cell* **22**, 2749–2767 (2010).
59. Jefferson, R. A., Kavanagh, T. A. & Bevan, M. W. GUS fusions: beta-glucuronidase as a sensitive and versatile gene fusion marker in higher plants. *EMBO J.* **6**, 3901–3907 (1987).
60. Peterson, G. L. A simplification of the protein assay method of Lowry *et al.* which is more generally applicable. *Analytical Biochem.* **83**, 346–356 (1977).
61. Buer, C. S. & Muday, G. K. The transparent testa4 mutation prevents flavonoid synthesis and alters auxin transport and the response of Arabidopsis roots to gravity and light. *Plant Cell* **16**, 1191–1205 (2004).

## Acknowledgments

This work was supported by the Natural Science Foundation of China (NSFC No. 31400246), the China Postdoctoral Science Foundation (No. 2014M562453) and Northwest A&F University basic research Foundation (No. 2014YB039). We thank professor Yun Xiang (Lanzhou University, Lanzhou, China) for *capa*, *capb* and *prf3* seeds.

## Author contributions

J.S.L. and H.L.J. designed research; J.S.L. and H.L.J. performed research; T.T.F. and Y.F.H. constructed transgenic plants; J.S.L., H.L.J., T.T.F. and Y.F.H. analyzed data; and J.S.L. and H.L.J. wrote the paper.

## Additional information

Supplementary information accompanies this paper at <http://www.nature.com/scientificreports>

**Competing financial interests:** The authors declare no competing financial interests.

**How to cite this article:** Jia, H., Hu, Y., Fan, T. & Li, J. Hydrogen sulfide modulates actin-dependent auxin transport via regulating ABPs results in changing of root development in Arabidopsis. *Sci. Rep.* **5**, 8251; DOI:10.1038/srep08251 (2015).



This work is licensed under a Creative Commons Attribution 4.0 International License. The images or other third party material in this article are included in the article's Creative Commons license, unless indicated otherwise in the credit line; if the material is not included under the Creative Commons license, users will need to obtain permission from the license holder in order to reproduce the material. To view a copy of this license, visit <http://creativecommons.org/licenses/by/4.0/>